

# Palaeoseismologic and geomorphic investigations along the middle portion of the Ovindoli-Pezza Fault (Central Italy)

Giuliana D'Addezio(\*), Daniela Pantosti and Paolo Marco De Martini  
*Istituto Nazionale di Geofisica, Roma, Italy*

## Abstract

This paper presents the results of a detailed investigation performed along the central part of the Ovindoli-Pezza Fault with the aim of improving our understanding of the seismic behaviour of this fault within Central Italy seismogenesis. Results of the trenching investigations we performed across the central part of the fault confirm and strengthen the results obtained at other sites located in the northern part. There is clear evidence that the two most recent surface faulting events occurred within the same interval of time at the different trench sites and thus, at least during these two events, the fault was activated for its entire length. The most recent surface faulting event occurred between 860 and 1300 A.D. Geomorphic and microtopographic investigations indicate that although the trace of the fault shows an important bend, the kinematics of the fault seem to be prevalently normal, consistent with the other seismogenic faults that accommodate the NE-SW extension in this part of the Apennines. The maximum horizontal movement derived using geomorphic methods along the central part of the Ovindoli-Pezza Fault did not exceed 30% of the vertical movement. Slip rate and average recurrence interval were obtained using data both from trenching and Late Pleistocene-Holocene geomorphology. Resulting slip rate ranges between 0.7 and 1.2 mm/year whereas the average recurrence time varies between 1000 and 3000 years.

**Key words** *active fault – geomorphology – palaeoseismology – microtopography – Central Italy*

## 1. Introduction

The Ovindoli-Pezza fault is an active, 20 km-long fault (fig. 1), located along the Apennine seismogenic belt where most of the large Italian earthquakes occur (Valensise *et al.*, 1993). This fault shows prevalent dip-slip movement that is particularly clear in the northern part, where it crops out as a WNW-trending, south-facing scarp that displaces Holocene fans, slope debris, late Pleistocene moraine and fluvio-glacial deposits by as much

as 18 m (Biasini, 1966; Giraudi, 1989; Cinti *et al.*, 1992a,b) (see table I). In the central part, the fault strike changes to NNW; in this portion the fault displaces, with a back-dipping geometry, Late Pleistocene and Holocene fluvio-glacial fan and moraine deposits. Frequently the fault trace coincides with pre-existing thrusts contact (fig. 1). On the basis of aerial photograph interpretation, slip along this portion of the fault was previously inferred to be both dip and strike (Biasini, 1966; Giraudi, 1989) (see table I). The southern part of the fault appears only as a geomorphic lineament (fig. 1) and it does not intersect any Quaternary or Holocene deposit.

Trenching investigations performed along the northern section of the Ovindoli-Pezza Fault at Piano di Pezza (sites A and B in fig. 1) showed that this is a seismogenic fault and

(\*) e-mail: daddezio @ ing750.ingrm.it

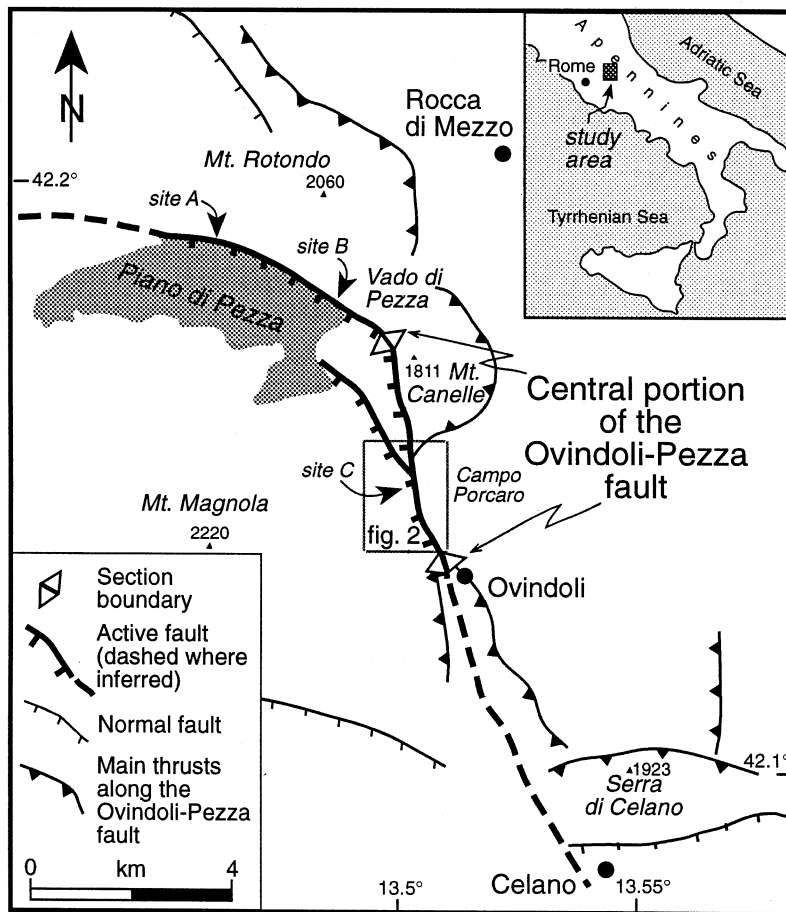


**Fig. 1.** Map of the Ovindoli-Pezza Fault and location of the trench sites. Most of the fault runs very close to the main thrust along which Mesozoic limestone and dolomite of the Magnola range overlie Miocene terrigenous units. Section boundaries delineate the three parts of the fault that have a different geometry or geomorphic expression: the northern, central, and southern parts.

provided the first information regarding the fault's slip rates and recurrence for large earthquakes (Cinti *et al.*, 1992b; Pantosti *et al.*, 1996).

The geometry of the Ovindoli-Pezza Fault, with a change in strike of about 60°, and its vicinity to a thrust contact related to past compressional activity (fig. 1), was interpreted as evidence of fault complexity. In fact, as already mentioned, some authors hypothesized that (1) even if in the northern part the fault

is prevalently normal, horizontal movement would prevail in the central part (Giraudi, 1989; 1992; Michetti, 1994), and (2) the fault reactivated the old low-angle compressional structures (Biasini, 1966; Michetti, 1994). However, the fault setting is similar all along the fault length and is characterized by a distinct graben formed between a main, several meter-high scarp and a well exposed antithetic fault. At Piano di Pezza (fig. 1), prevalent dip-slip movement is recognized on the basis of

**Table I.** Summary of the estimates of total displacement and type of movement along the northern and central part of the Ovindoli-Pezza Fault proposed by different authors on a geomorphic basis.

Reference	Piano di Pezza	Campo Porcaro
Biasini (1966)	10 m vertical (Late Quaternary)	6 m vertical ( $< 7000$ years) 8-9 m vertical (Late Quaternary)
Giraudi (1989)	7-9 m vertical ( $< 16000$ )	7-8 m vertical 12-15 left-lateral ( $< 7000$ years) 17 m vertical 65-70 m left-lateral (18000 years)
Cinti <i>et al.</i> (1992a)	max 18 m vertical ( $< 16000$ years)	

microtopographic investigations along the scarp and also confirmed by the geometry of the structures observed in several exploratory trenches (Cinti *et al.*, 1992a).

Prevalent normal faulting across the Ovindoli-Pezza Fault also agrees with the observation that, as suggested by faults that produced large earthquakes during this century, the present tectonic regime in the Central Apennines is dominated by NE-SW extension with faulting on  $40^\circ$  to  $70^\circ$  dipping planar faults located between a depth of 12-15 km and the surface (Valensise *et al.*, 1993). In this light, the understanding of the kinematics and behavior of the Ovindoli-Pezza Fault can help to improve our knowledge of Apennine seismogenesis.

In this paper we present the detailed investigations we developed along the central section of the fault. We focused on this part of the fault, on the one hand, because it was the subject of divergencies and open questions, on the other, because it contains favorable sites for trenching and microtopographic investigations (site C in fig. 1). Geomorphic and microtopographic studies are used to test fault geometry and kinematics, whereas trenching investigations help to constrain the seismic behavior of the fault.

## 2. The central section of the Ovindoli-Pezza Fault

Although at present this portion of the fault is highly modified by human activity, geomorphic analyses were possible because some patches of land remained undisturbed. In addition, aerial photographs pre-dating the landscape modification (year 1954, 1:33000 scale) were available (fig. 2). The central part of the fault appears as a  $N165^\circ$  scarp that, to the north bounds the southwestern slope of Mt. Canelle forming a double crest in the bedrock, and to the south displaces Late Pleistocene and Holocene deposits and Tertiary bedrock. Here, the fault is faced by an antithetic scarp that displaces the Quaternary deposits and, with the main fault, forms a distinct graben. Locally, the main scarp forms a small bench that can be related to multiple events of deformation on a single fault or to several fault splays. Part of this fault section is also a secondary, 2 km-long fault branch that splays from the main fault north of Campo Porcaro and bounds to the northeast the triangular basin of Campo di Via (figs. 1 and 2).

The most recent geomorphic elements clearly involved in faulting are two streams de-

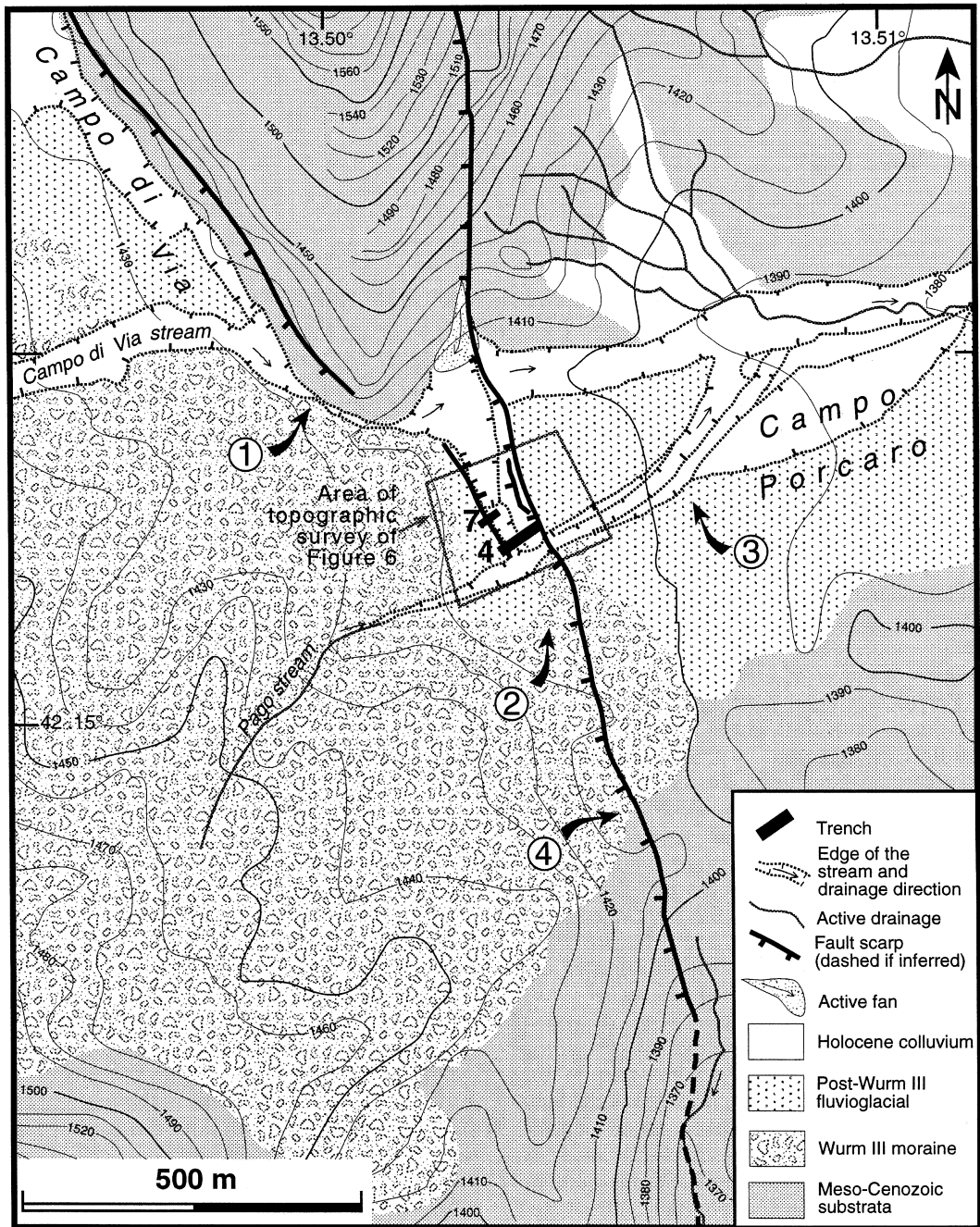


**Fig. 2.** Geomorphic map of the central part of the Ovindoli-Pezza Fault from field survey and aerial photo interpretation. Black rectangles are the exploratory trenches opened across the main and antithetic scarps (numbers refer to those used in the text).

scending the Magnola range: the Campo di Via and the Pago streams (figs. 1 and 2). These streams are incised into the two opposite flanks of a wide fluvioglacial fan, at present are ephemeral and are dammed by the fault. Damming and ponding against the fault scarps into the graben, is clearly suggested by the erosional edges (that could be interpreted as lake shorelines) that surround the graben itself (fig. 2). On the basis of aerial photos, Biasini (1966) and Giraudi (1989, 1992) estimated a vertical displacement of the Pago stream bed (considered to be younger than 7000 years) of 6 m and 7-8 m, respectively (see table I). Based on topographic profiling, we evaluate a net vertical displacement of this stream ranging

between 5.5 and 10 m. The lowest displacement is calculated assuming the extreme, but unlikely, possibility that the original profile of the stream was horizontal (fig. 3). Using aerial photos, Giraudi (1989) suggests that, in addition to the vertical displacement, the right edge of the Pago stream bed records a sinistral offset of 12-15 m (see table I). However, fig. 2 shows that the stream incisions are influenced not only by the fault activity but also by the pre-existing topography and changes in lithology. For instance, the Campo di Via stream formed a sharp bend southward (arrow 1 in fig. 2) because of the presence of the carbonate bedrock, whereas the Pago stream was probably restrained by part of the arcuated moraine

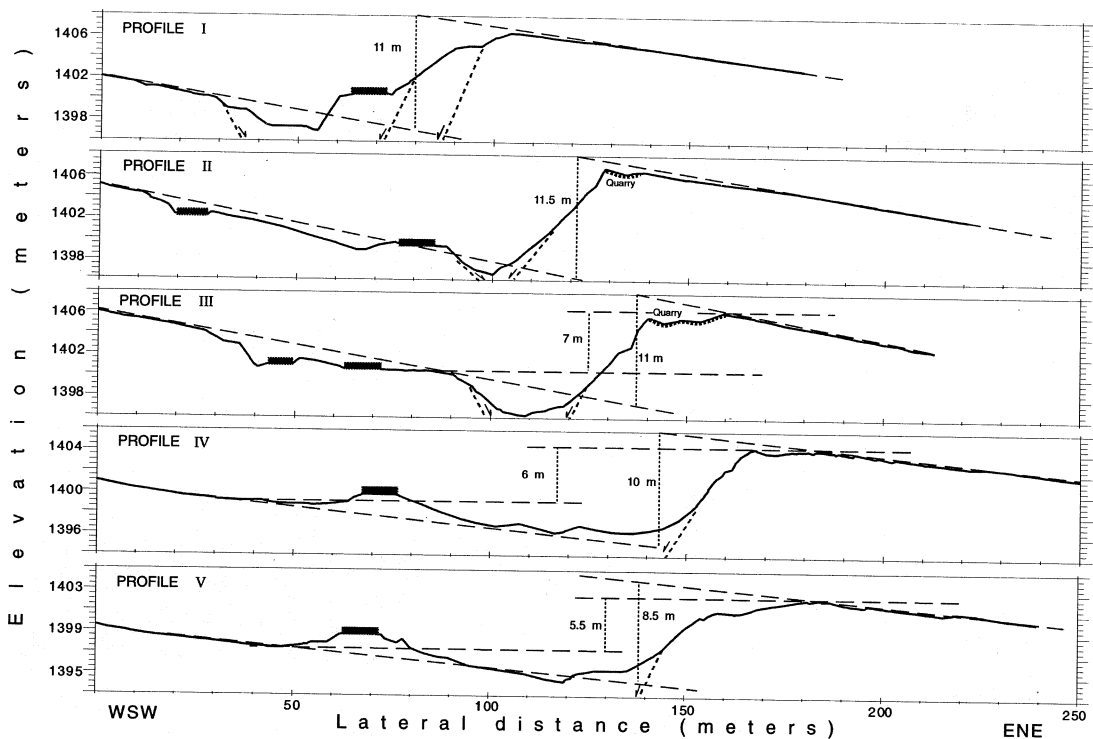


**Fig. 3.** Topographic profiles across the main and antithetic scarps at Campo Porcaro (site C), location of profiles is shown in fig. 6. Minimum and maximum vertical separations across the scarp are evaluated for the fluvioglacial fan (profiles I, II, and III) and the Pago stream (profiles IV and V). The minimum vertical separation is measured assuming an original horizontal surface. The thick grey bars indicate the intersection between the profiles and the road.



front that controlled not only the right edge of the stream but also the geometry of the fluvio-glacial fan (arrow 2 in fig. 2). Conversely, the left edge of the Pago stream seems to be more independent from previous topography and does not show any substantial lateral offset. The ambiguity due to the non-uniqueness of the interpretation of the geometry of the stream edges is even increased because of the distance between the two parts of the stream that can be matched by using aerial photos (up to 80 m). Within this distance the stream could be naturally diverted, especially because of the natural flattening of the stream profile from the steep slopes to the west toward the open valley to the east (Campo Porcaro in fig. 2). From a different perspective, some information regard-

ing possible lateral movement of this portion of the fault could be derived from the study of the drainage of Pago stream in the footwall of the fault. The reconstruction of the edges of the stream, that incises the well preserved fluvio-glacial fan forming the Campo Porcaro plain, shows a progressive deviation northward where it is captured by the Campo di Via stream (arrow 3 in fig. 2). Generally, this would support sinistral offset along the fault. However, considering that: 1) the fault has a back-dipping geometry with respect to the topography; 2) the stream here flows through a quite flat area, and 3) the transversal profile of the fan is generally convex and symmetric with respect to the apex, the northward deviation of the Pago stream would suggest a dextral com-



**Fig. 4.** View of the south wall of trench 4. The photograph shows the main fault zone and the small graben formed in front of it (in fig. 5a is located between m 8 and 13). Units are named as in fig. 5a. The black arrow indicates the main fault scarp.

ponent of movement on the fault and would exclude a sinistral offset. In fact, a sinistral component of the movement would have produced a diversion of the Pago to the south of its incision because this area would correspond to the lowest topography. However, considering the uncertainties of these reconstructions in a glacial-alluvial environment, on the basis of aerial photo interpretation and field survey there is a non-uniqueness of the interpretation.

The fluvioglacial fan, that post-dates the last glaciation (Wurm III, highest peak 18000, Cassoli *et al.*, 1986), is probably younger than 10000 (Giraudi, 1989). On the basis of topographic profiling we estimate a vertical displacement of 7 to 11.5 m for the top of the fan (fig. 3). As the original shape of the fan was irregular due to the topography it was overlying, it cannot be used to study horizontal offset. Moraines related to the Wurm III glaciation (about 18000 year old, Cassoli *et al.*, 1986) crop out extensively in the area and are intersected by the fault. Based on aerial photo analysis, Giraudi (1989) evaluated 17 m of total vertical displacement for the moraines. Moreover, matching an indentation between two juxtaposed arcuate fronts of the moraine (arrow 4 in fig. 2), he evaluated a sinistral offset of 65-70 m (see table I). Considering that the depositional characteristics of the frontal moraines normally include a sequence of arcuate fronts, these estimates appear not sufficiently supported.

### 3. Trenching

We selected a site favorable for trenching just north of the Pago stream (fig. 2) where the main and antithetic scarps are clearly exposed. At this site the Pago stream is dammed by the fault which strictly controlled also location and type of deposition. Because of that, this site appeared promising for intercepting with excavation young faulted deposits. We excavated three trenches across the scarps: trench 4 cut both the main and antithetic scarps, trench 6 cut only the main scarp but intercepted deposits highly disturbed by human activities,

and trench 7 cut only the antithetic fault (fig. 2). Trenches 4 and 7 were logged in detail at a 1:20 scale. We divided the stratigraphic sequence exposed in each trench into units, that are indicated by a letter followed by a number that refers to the number of the trench the unit belongs to (*i.e.*, units from trench 7 are always indicated by a 7). Units that are indicated with the same letter belong to the same sedimentary event.

To obtain age constraints on the stratigraphy, paleosols and charcoal fragments were collected and dated using radiocarbon techniques (both conventional and Accelerator Mass Spectrometry). The measured ages were corrected for possible contamination on the basis of  $^{12}\text{C}/^{13}\text{C}$  ratio, and for changes of  $^{12}\text{C}/^{14}\text{C}$  ratio in the atmosphere (Pearson *et al.*, 1986, 1993; Stuiver and Becker, 1993). In the text and figures the corrected age of the samples is always adjusted to the nearest decade and given as  $2\sigma$  interval according to the calibration program CalibETH Niklaus (1994).

Trench 4 is about 32 m long and 3.5 m deep; it exposes a sedimentary sequence composed of alluvial and colluvial deposits overlying fluvioglacial gravel and includes some paleosols (figs. 4 and 5a). The stratigraphic sequence is divided into seven units; units h4 to e4 are intensely faulted, whereas units d4, c4, and the active soil a4 bury the faulted sequence. Dating of several samples from unit e4 (paleosols and charcoal fragments) yielded a weighted mean age of 650-760 A.D., whereas dating of paleosol g4 (mean residence time, MRT, date) yields an age of 1890-1600 B.C. (fig. 5a).

As a whole, the structure exposed in the trench forms a main 30 m-wide graben bounded by several steep (70-80°) synthetic and antithetic faults that duplicate the present topography. A secondary, small but distinct graben formed within the main graben at the base of the main scarp (m 8-13 of fig. 5a). This secondary graben is bounded by a main synthetic fault zone and some antithetic faults and represents the preferred location for alluvial channels. At present, the graben is buried under a thick cover of colluvium (units c4 and

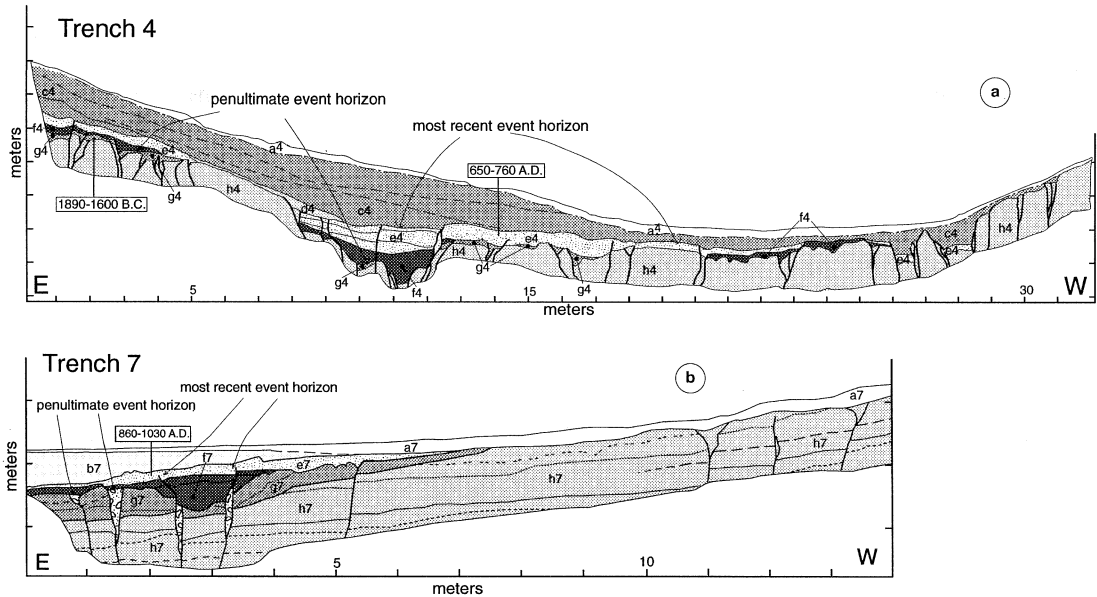


**Fig. 5a,b.** Simplified logs of trenches 4 and 7 (from 1:20 detailed mapping). Rectangles enclose the ages obtained from radiocarbon dating (see text for details). a) Trench 4 symbols: a4 = dark brown organic soil; c4 = loose gravel normally graded, interbedded with sandy and silty layers (scarp-derived deposit); d4 = sparse medium size gravel in rich organic matrix (colluvial wedge); e4 = brown silt and sand interbedded with thin layers of fine gravel and sparse lenses of coarse gravel; f4 = reddish massive clay and silt containing rare medium to coarse gravel wedges; g4 = fine angular gravel in a silty reddish matrix; h4 = white fine to coarse calcareous gravel in a sandy matrix (fluvioglacial fan deposits). b) Trench 7, symbols: a7 = active soil; b7 = green clay; e7 = brown paleosol developed on unit f7; f7 = organic rich alluvial channels; g7 = sandy gravely orange-brown alluvial channels; h7 = white fine to coarse calcareous gravel in a sandy matrix (fluvioglacial fan deposits).

d4); the presence of this thick cover on the footwall of the main fault zone, along with the presence of a bench in the scarp profile, suggest that one other important synthetic fault zone could be located further E, toward the top of the scarp (figs. 4 and 5a). For safety reasons and tree preservation we were not able to extend the trench through it.

The structures exposed in this trench do not show evidence for horizontal movement. In addition, the trenches opened along the northern part of the fault at Piano di Pezza (sites A and B in fig. 1), showed a similar setting with a wide graben bounded by a series of synthetic and antithetic faults (Cinti *et al.*, 1992b; Pantosti *et al.*, 1996). This comparison suggests that the type of movement on the northern and

central part of the fault is consistent. Thus, because at Piano di Pezza the movement is well constrained as prevalently dip-slip, we would expect the central part of the fault to behave similarly.

Trench 7 is about 14 m long and 2 m deep; it exposes alluvial channel and fluvioglacial deposits with some interbedded paleosols (fig. 5b). The sequence is divided into 6 units. Units h7 to e7 are clearly faulted whereas unit b7 and the present-day soil horizon appear undisturbed. Radiocarbon dating (MRT) of paleosol e7 yields an age of 860-1030 A.D. The stratigraphic sequence is faulted by several antithetic faults and a couple of synthetic faults that in general show a few centimeters of dis-



placement. These structures produce a broad warping of the topographic surface and form a depressed area that also includes a small graben (m 2 to 3.5 in fig. 5b) that controlled the location of the alluvial channels (units g7 and f7).

Stratigraphic relations and structures exposed in the trenches show evidence for at least two surface faulting events in this part of the Ovindoli-Pezza Fault (fig. 5a,b). The last faulted units in the trenches are e4 and e7. Therefore, the upper part of these units can be interpreted as the topographic surface at the time of the occurrence of the most recent event (*i.e.*, event horizon). The age of unit e7 is younger than that obtained for e4 so the former is used to constrain the maximum age for the most recent event that should have occurred after 860 A.D. Evidence for the most recent event in trench 4 is also provided by the well developed scarp-derived colluvial wedge (units c4-d4) formed in correspondence to the main synthetic fault zone (m 5-10 of fig. 5a). A minimum amount of net vertical displacement on the main fault zone of about 2 m was derived in trench 4 (fig. 5a). This should be considered a minimum because, as already discussed, another important fault zone could be located further east on the scarp.

Evidence for a penultimate event is found in both trenches. In trench 4, this event is recognized mainly because: 1) unit g4 shows an angular unconformity (m 0-4 in fig. 5a) and a greater displacement with respect to units e4 and f4; 2) several faults terminate upward and are capped by unit f4; 3) the lower part of unit f4 is formed by localized, wedge-shaped gravel that is faulted by the most recent event (m 9-12 in fig. 5a) and is interpreted as a colluvial wedge post-dating a previous event. In trench 7 the penultimate event is defined by open fissures in units g7 and h7 that terminate upward, and are capped by units f7 and e7 (m 1-4 in fig. 5b). The event horizon for the penultimate event can be considered the top of units g4 and g7. At present we have only one dated sample from trench 4 that pre-dates the penultimate event. On this basis, we suggest that the penultimate event occurred between 1890 B.C. and 1030 A.D.

Comparing the timing of the events we obtained at this site with those from Piano di Pezza (sites A and B in fig. 1, Cinti *et al.*, 1992b; Pantosti *et al.*, 1996) we found a good correlation. This suggests, within the error of the available ages, that the central and northern part of the fault slipped jointly at least during the last two events.

#### 4. Microtopographic investigations

The geomorphic and trenching investigations we developed along the central part of the Ovindoli-Pezza fault do not show any definite evidence for horizontal movement on this fault. Normal faulting seems to prevail. However, to study the proposed important sinistral slip on this part of the fault (Giraudi, 1989), we reconstructed in detail the fault-related topography of the Pago stream at Campo Porcaro using an electronic geodimeter (total station). Microtopographic mapping represents a valuable tool for understanding the geometry and kinematics of active structures because it highlights all the subtle geomorphic elements that may have recorded slip on the fault. Our microtopographic survey covers an area of about 250 m<sup>2</sup> (figs. 2 and 6). Data were processed using contouring programs in order to obtain the maps of figs. 6 and 7a,b. The map was used to quantify the scale of the deformation recorded by geomorphic elements which cannot be resolved on the basis of the official mapping (1:10000) or field survey. Notwithstanding human modification, figs. 6 and 7 show clearly the main antithetic faults that cut the fluvio-glacial fan and the Pago stream. The main fault exhibits a little bench at two-thirds of its height that was also apparent in aerial photos (fig. 2), which could be evidence of a second fault splay. The shape of the fluvio-glacial fan is very regular in the mapped area and the original surface was reconstructed by removing the vertical deformation due to the main and antithetic faults. The Pago stream offers a unique possibility to investigate possible horizontal movement at this site even though we have to take into account that the stream could have been naturally diverted

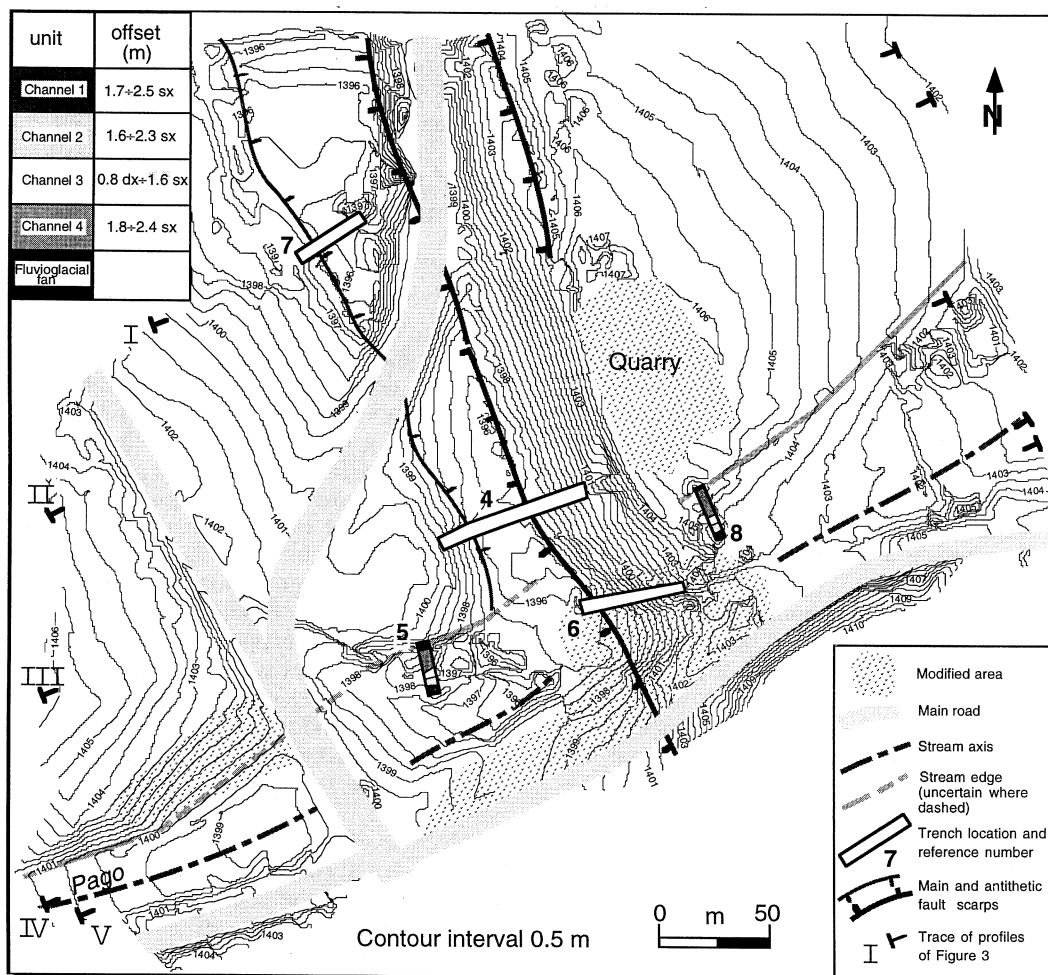


**Fig. 6.** Topographic map of site C at Campo Porcaro based on 2200 total station points. The total station is an electronic geodimeter that measures and digitizes elevation and coordinates of points on the topographic surface. The figure also shows the precise location of the cut and fill channels from the Pago stream as exposed in trenches 5 and 8 (see fig. 8). Individual channel offset is used to investigate possible horizontal movement on this part of the fault (see upper left inset).

because of: 1) fault's location and activity; 2) change in slope from the steep mountain range to the open valley; 3) presence of irregular moraine fronts. Overall, the Pago stream axis appears rectilinear without any clear evidence for horizontal offset. This is particularly true when considering those portions of the stream that are away from the near fault disturbances

and from the most modified area. To investigate the exact location and the evolution of the left edge of the Pago stream in more detail, we opened two scarp-parallel trenches: trench 5 on the hanging wall, and trench 8 on the footwall (figs. 6 and 8). The two trenches show a similar stratigraphy that is composed of a sequence of alluvial channels. The oldest channel incises

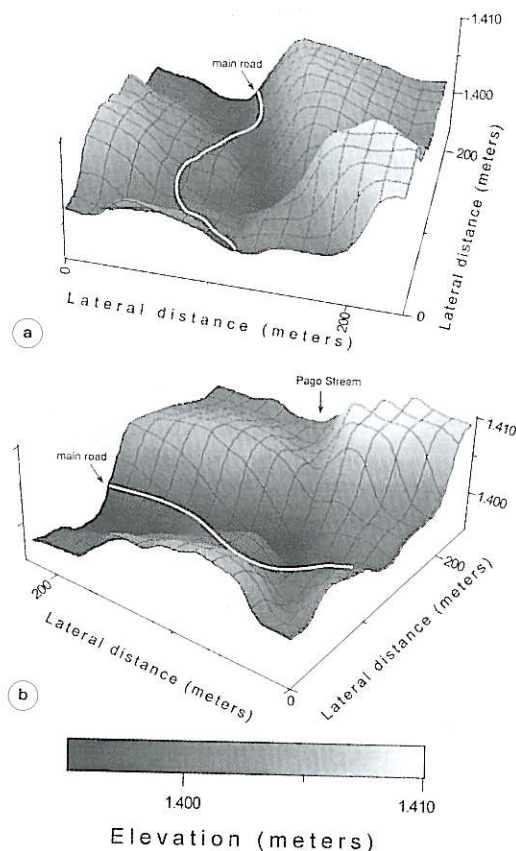


Fig. 7a,b. 3D views of site C derived from microtopographic data: a) view to the north; b) view to the east.

directly into the fluvio-glacial fan and coincides with the left edge of the Pago stream in the topography. The other channels migrate progressively toward the center of the stream (fig. 8). Grain size of deposits, width, and thickness of the channels decrease proportionally with youthfulness. We located the position of the channels of trenches 5 and 8 in the topographic map of fig. 6 to correlate them precisely across the fault. Projecting the edge of individual channels across the fault, and taking into account the uncertainties related to natural diversions, we estimate possible horizontal offset ranging between 2.5 m sinistral and 0.8 m dextral.

## 5. Conclusions

The complex geometry of the Ovindoli-Pezza Fault with a change in strike of up to  $60^\circ$ , was considered by some authors as evidence for different behavior of the two differently striking parts of the fault. This interpretation could imply not only different kinematics along the fault but also independent timing and behavior in terms of strain release in the two parts of the fault. In this study, geomorphic, microtopographic, and trenching investigations were performed along the central part of the Ovindoli-Pezza Fault and compared to the results obtained at different sites along the fault. Despite the complexity of the fault's trace, the structures exposed in the trenches and the setting of the scarps indicate a good consistency along the fault length, show strong similarities in all the sites we investigated, and suggest a prevalent vertical movement. Moreover, the microtopographic mapping of geomorphic features displaced by the fault at Campo Porcaro confirms that the horizontal movement in the central part of the fault is certainly secondary to the normal component. By reconstructing the evolution of the incision of the Pago stream and by using two fault parallel trenches we estimated a possible horizontal movement for the past 7000 years ranging between 0.8 m dextral and 2.5 m sinistral (fig. 6). This, compared to the vertical displacement accumulated during the same period of 5.5-10 m by the stream (fig. 4), indicates that the horizontal movement does not exceed 30% of the vertical in the central part of the Ovindoli-Pezza Fault.

The trenches excavated at Campo Porcaro (site C) show clear evidence for two palaeo-earthquakes that correspond in terms of age (within the error) and size of deformation to the two most recent surface faulting palaeo-earthquakes recognized at sites A and B of Piano di Pezza (fig. 1). This indicates that at least during these events the fault slipped conjointly. Based on the age constraints, obtained by radiocarbon dating on charcoal fragments and paleosols obtained from all the trench sites (Pantosti *et al.*, 1996), and on historical considerations (D'Addezio *et al.*, 1995) we set the age of occurrence of the most recent event be-

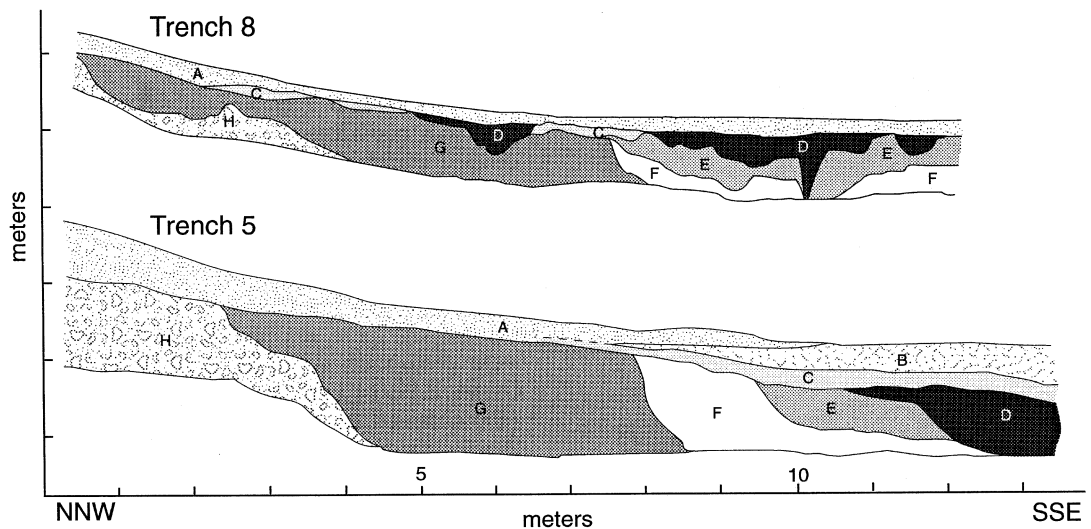


**Fig. 8.** Simplified logs of the fault-parallel trenches 5 and 8 at Campo Porcaro site. Symbols: A = active soil; B = massive gray clay; C = brown silty soil; D = channel 1: red silt with carbonate pebbles; E = channel 2: orange-brown sandy fine gravel, containing frequent sand lenses; F = channel 3: white sandy medium gravel; G = channel 4: reddish sandy gravel; H = fluvio-glacial fan deposits.

tween 860 A.D. and 1300 A.D. and of the penultimate around 1900 B.C. Merging the results from trenching with the detailed geomorphic investigation we evaluate the main parameters representative of the seismogenic behavior of this fault: slip rate and recurrence time. The slip rate ranges from 0.8-1 mm/yr from the trenches to 0.7-1.2 mm/yr calculated on the displacement of the Pago stream bed and on the surface of the fluvio-glacial fan. The average recurrence time from the trenches is not well constrained but, based on the reconstruction of displaced geomorphic elements, yields a range between 1000 and 3000 years. On the other hand, these values are confirmed by the long term slip rate from cumulative displacement of geomorphic features considering periodic strain release.

In this light, the Ovindoli-Pezza Fault appears to be fully consistent, in terms of kinematics, rates of deformation, and frequency of earthquakes, with the other main seismogenic faults that accommodate NE-SW extension across the Apennines (Valensise *et al.*, 1993).

### Acknowledgements

We wish to thank the local Authorities and Mr. G. Bortolotti for allowing us to work at this site and all the people that participated in the total station surveying and trench study for their valuable collaboration. We are also grateful to Richard Collier and Gerald Michel for their thorough reviews and for their valuable comments and suggestions.

### REFERENCES

- BIASINI A. (1966): Elementi morfotettonici, tratti da un rilievo fotogeologico al margine dell'altipiano di Ovindoli, *Geologica Romana*, **5**, 303-312.
- CASSOLI, A., L. CORDA, C. LODOLI, A. MALATESTA, M.V. MOLARONI and A. RUGGERI (1986): Il glacialismo quaternario del gruppo Velino-Ocre-Sirente, *Mem. Soc. Geol. It.*, **35**, 855-867.
- CINTI F. R., G. D'ADDEZIO, D. PANTOSTI and J. HAMILTON (1992a): Ricostruzione topografica di dettaglio della scarpata di faglia del Piano di Pezza, Abruzzo, *Studi Geologici Camerti*, 1992/1, 115-122.
- CINTI F.R., D. PANTOSTI, G. D'ADDEZIO and P.M. DE MARTINI (1992b): Paleosismicità della faglia Ovindoli-

- Pezza (Abruzzo), in *Atti XI Convegno GNGTS*, Roma, 331-342.
- D'ADDEZIO, G., F.R. CINTI and D. PANTOSTI (1995): A large unknown historical earthquake in the Abruzzi region (Central Italy): combination of geological and historical data, *Annali di Geofisica*, **38**, 491-501.
- GIRAUDI, C. (1989): Datazione con metodi geologici delle scarpate di faglia post-glaciali di Ovindoli-Piano di Pezza (Abruzzo-Italia centrale): implicazioni, *Mem. Soc. Geol. It.*, **42**, 29-39.
- GIRAUDI, C. (1992): Segnalazione di scarpate di faglia tardo-pleistoceniche sui Monti della Magnola (Massiccio del Velino - Abruzzo), *Il Quaternario*, **5** (1), 27-32.
- MICHETTI, A.M. (1994): Coseismic surface displacement vs. Magnitude: relationships from paleoseismological analyses in the Central Apennines, Italy, in *Proceedings of the CRCM'93*, Kobe, December 6-11, 1993, 375-380.
- NIKLAUS, T.R. (1994): CalibETH calibration program, version 1.5. ETH, Institute of Particle Physics, Zurich.
- PANTOSTI, D., G. D'ADDEZIO and F.R. CINTI (1996): Paleoseismicity of the Ovindoli-Pezza Fault (Central Apennines, Italy): geological evidence for a large unknown Middle Age earthquake, *J. Geophys. Res.*, **101** (B3), 5937-5959.
- PEARSON, G.W., J.R. PILCHER, M.G.L. BAILLIE, D.M. CORBET and F. QUA (1986): High-precision  $^{14}\text{C}$  measurements of Irish Oaks to show the natural  $^{14}\text{C}$  variations from A.D. 1840-5210 B.C., *Radiocarbon*, **28** (2B), 911-934.
- PEARSON, G.W., B. BECKER and F. QUA (1993). High-precision  $^{14}\text{C}$  measurements of Irish Oaks to show the natural  $^{14}\text{C}$  variations from 7890 to 5000 B.C., *Radiocarbon*, **35** (1), 93-104.
- STUIVER M. and B. BECKER (1993): High-precision Decadal calibration of radiocarbon time-scale, A.D. 1950-6000 B.C., *Radiocarbon*, **35** (1), 35-66.
- VALENSISE, G., D. PANTOSTI, G. D'ADDEZIO, F.R. CINTI and L. CUCCI (1993): L'identificazione e la caratterizzazione di faglie sismogenetiche nell'Appennino Centro-Meridionale e nell'Arco Calabro: nuovi risultati e ipotesi interpretative, in *Atti XII Convegno GNGTS*, Roma, 331-342.